Science of the Total Environment 869 (2023) 161647

Contents lists available at ScienceDirect

Science of the Total Environment

journal homepage: www.elsevier.com/locate/scitotenv

Storm pulse responses of fluvial organic carbon to seasonal source supply and transport controls in a midwestern agricultural watershed

Tingyu Hou [a], Neal E. Blair [b], A.N. Thanos Papanicolaou [c], Timothy R. Filley [a,*]

[a] Department of Geography and Environmental Sustainability, the School of Geosciences, University of Oklahoma, Norman, OK, USA
[b] Departments of Civil and Environmental Engineering, and Earth and Planetary Sciences, Northwestern University, Evanston, IL, USA
[c] National Laboratory for Agriculture and the Environment, Ames, IA 50011, USA

HIGHLIGHTS

- High-resolution particulate and dissolved organic carbon dynamics of six storms monitored
- Export of storm-induced particulate organic carbon export consistently exceeds that of dissolved.
- Rapid liberation of easily erodible organic carbon during the bare soil period in October
- A progressive leaching of dissolved organic carbon during rapid crop growth period in June/July
- Largest difference between particulate and dissolved organic carbon export in June/July events

GRAPHICAL ABSTRACT

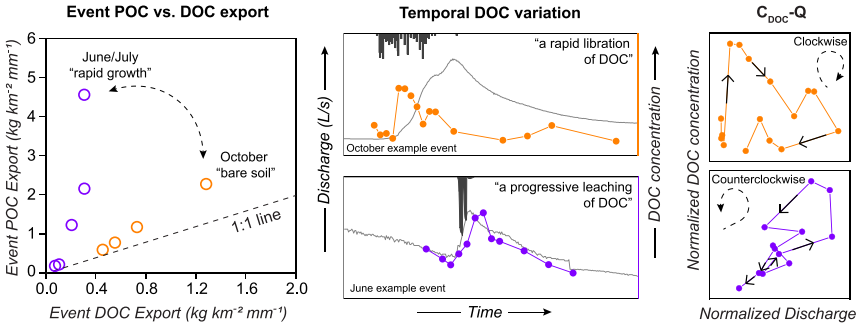

ARTICLE INFO

Editor: Christian Herrera

Keywords:
Fluvial OC export
DOC
POC
Storm events
High-resolution monitoring

ABSTRACT

Storm events are the primary mechanisms of delivering fluvial organic carbon (OC) in both dissolved (DOC) and particulate (POC) forms but their sources and flow pathways can vary with seasonal land use and weather. Within the low relief and poorly drained landscapes of a predominantly agricultural watershed in Eastern Iowa, six storm events were monitored for DOC and POC concentrations over a two hydrological year period in order to investigate the export mechanisms, landscape connectivity, and hydro-climatological controls of fluvial OC under representative events and associated management practices. Event-driven dynamics favored POC over DOC, where POC accounted for 54–94 % of total OC export during events, highlighting a sampling-driven bias against POC in the absence of event monitoring. The disparity between POC and DOC export exhibited a seasonal effect, where the POC:DOC export ratio was low (1.3–1.7) for October events while June/July events yielded a much higher value (up to a value of 14.7). The relationships between event DOC and POC export, Normalized Difference Vegetation Index of landscapes, and antecedent wetness conditions suggest a strong interaction or competing influences between vegetation coverage and runoff-generation threshold. While we recognize the low statistical power of the limited data set ($n = 6$), the storm events could be binned into two clusters: a "bare soil" period and a crop "rapid growth" period. Specifically, intra-storm variations in OC concentration and concentration-discharge (C-Q) hysteresis patterns demonstrated a seasonally-dependent access to contributing OC sources, which can be viewed as the rapid liberation of DOC during the "bare soil" period, and a progressive leaching of terrestrial DOC during the "rapid growth" period. Although high resolution event monitoring of fluvial carbon is rare this work highlights the importance of such efforts to predict C sourcing and transformation in inland water systems under variable land use and across seasons.

* Corresponding author at: Department of Geography and Environmental Sustainability, University of Oklahoma, 100 East Boyd Street, Norman, OK 73019, USA.
E-mail address: filley@ou.edu (T.R. Filley).

http://dx.doi.org/10.1016/j.scitotenv.2023.161647
Received 12 September 2022; Received in revised form 12 December 2022; Accepted 12 January 2023
Available online 18 January 2023

1. Introduction

Fluvial organic carbon (OC), which exists along a dynamic continuum of dissolved (DOC) and particulate (POC) forms, is an important, albeit poorly understood, component of the global carbon cycle (Cole et al., 2007; Drake et al., 2018). The amount, composition, and reactivity of DOC and POC within fluvial networks are highly variable in space and time (Dalzell et al., 2007; Hernes et al., 2008; Wilson and Xenopoulos, 2009; Lambert et al., 2017), and much of this variability comes down to the interplay among the mechanisms of creation, mobilization, and subsequent transport (Battin et al., 2008). Understanding the relative contribution of POC and DOC in streams and how they vary in response to hydrological regimes is critical for identifying and modeling the responsible processes and drivers (Pawson et al., 2012). Specifically, the transport of soil-derived POC to streams is thought to require a higher transfer energy threshold than DOC (Jeong et al., 2012; Dhillon and Inamdar, 2014) as much allochthonous POC must first be detached from soil aggregates (Hou et al., 2021) and/or entrained from land surface by shear fluid action (Battin et al., 2008; Hilton et al., 2010). In contrast, DOC creation or liberation and subsequent mobilization to streams is a function of connected surface and subsurafce flow paths that integrate dissolved carbon from sources including root exudates, microbial metabolites, desorption from soil mineral surfaces or soil aggregates, and leaching from litter decay, algae, and plants, but all susceptible to alteration based on the rates of microbial decomposition within the flowpath (Sanderman et al., 2009; Inamdar et al., 2011).

While numerous studies have focused on fluvial OC export at relatively large temporal intervals of a predetermined frequency, such as seasonal and/or annual monitoring usually at the watershed outlet (e.g., Dalzell et al., 2005; Cai et al., 2008; Alvarez-Cobelas et al., 2012), few have reported high-resolution sampling during storm events (e.g., Lambert et al., 2014; Blair et al., 2021), and even fewer on relationships between event DOC and POC export across the drainage network (e.g., Dalzell et al., 2007; Oeurng et al., 2011; Dhillon and Inamdar, 2014). Storm events are the major driver of hydraulic forcing in a watershed, which can amplify POC and DOC delivery processes through raindrop-induced breakdown of soil aggregates and enhancement of overland runoff (Wacha et al., 2018, 2020). Recent studies have demonstrated how storm events are responsible for disproportionately greater export of terrestrial OC than baseflow periods (Raymond and Saiers, 2010; Dhillon and Inamdar, 2014). In an assessment of 31 small forested watersheds in the eastern US, it was reported that over 50 % of annual DOC was exported in large storms that made up only 5 % of the annual water events (Raymond and Saiers, 2010). Additionally, greater storm response of OC export was reported in agricultural landscapes within the U.S. Midwest for both POC and DOC where ~80 % of annual DOC export occurred during 20 % of the water year (Dalzell et al., 2007). Similarly, while discrete storms accounted for only 22 % of the water year in a large agricultural catchment in southwest France, these events accounted for 62 % and 76 % of total DOC and POC export, respectively (Oeurng et al., 2011).

The magnitude of the mobilization and export of OC within agricultural landscapes is a function, in part, of human-induced modifications that accelerate water and mass transfer (Raymond et al., 2008). Agricultural practices replace the dominant vegetation cover, physically disrupt soil structure, change surface roughness, and expose soils to rain and wind energy for long periods after tillage and harvest (Raymond et al., 2008; Elhakeem et al., 2018). One of the most significant impacts on OC mobilization and export dynamics in the US Midwestern agricultural regions may be the extensive, intentional hydraulic "modification" of the landscape through ditching and tile drain emplacement, altering surface and subsurface flow pathways (Dalzell et al., 2007; Blair et al., 2021). It is estimated that 84 % of continuously drained croplands in the US are in the upper Midwest and the drained area has increased dramatically, by approximately 14 %, in the last decade (USDA National Agricultural Statistics Service, 2017; Valayamkunnath et al., 2020). This enhanced drainage leads to a decrease in water residence time, an increase in infiltration rate (Schilling et al., 2018), and an increase in moisture deficit and runoff-generation threshold (Cain et al., 2022). It has been speculated that below-ground drainage can also increase the contribution of deeper soil OC pools to total OC export through enhanced oxidation of previously anaerobic soil C (Dalzell et al., 2007; Amado et al., 2017).

A variety of management, geomorphic, and weather-related drivers must be considered, such as thresholds of precipitation and antecedent soil wetness condition, when attempting to understand what controls the activation of the surface and subsurface transport pathways for POC and DOC in storms (Papanicolaou et al., 2015a, 2015b; Blair et al., 2021; Cain et al., 2022). Lambert et al. (2017) reported that agricultural management favors POC in terrestrial OC transfer, and suggested the reason is the increased soil erosion - consistent with greater sediment loading found in agricultural watersheds (Van Oost et al., 2007; Wilson et al., 2012; Abban et al., 2016). Our previous study utilized a high-resolution sampling scheme to assess POC dynamics from storm events in the Clear Creek Watershed (CCW) of eastern Iowa, a low-lying tile-drained Midwest agricultural watershed (Blair et al., 2021). That study attributed the major POC sources to in-stream production, upland surface soil erosion, and stream bank erosion that were delivered in a sequential process. While Blair et al. (2021) considered the contribution of tile drain to POC export as minor, tile drains may exert a greater influence on DOC export (Dalzell et al., 2011) particularly when storm events coincide with specific management practices (Battin et al., 2008).

Foundational conceptual models constructed for natural systems primarily attribute event-driven DOC sources the riparian upper soil horizons, where prolonged saturation is followed by drainage of OC-enriched pore water into a waterway (Royer et al., 2006). Given that tile drainage can quickly deliver OC into stream channels, thereby bypassing the riparian zone (Schilling et al., 2018), these models of how terrestrial OC is delivered into the fluvial network do not capture the "hydraulic plumbing" impacts that artificially drained agricultural landscapes have. Thus, knowledge gaps remain in our understanding of how storms in intensively managed agricultural landscapes in the US Midwest control OC export and influence the responses of surface and subsurface transport pathways of POC and DOC.

The work presented herein leverages our previous study of POC dynamics at CCW (Blair et al., 2021) by incorporating DOC monitoring from the same storm events and sampling sites within the drainage network to provide a more complete picture of the event-driven, fluvial OC export dynamics and associated relationships between event DOC and POC export under different mnagament. We investigated the interplay of management and hydro-climatological controls on hydraulic connectivity from contributing sources to flow transport into streams, covering storm events during representative time periods in agricultural management across a two-hydrological year period. We hypothesized that (1) Storm-derived high flow magnitiudes will yield a higher relative contribution of POC over DOC in total fluvial OC export; (2) The extent of the differential POC and DOC contribution to fluvial OC will depend upon management periods in an agricultural cycle with controls on crop growth stage, tillage, and soil exposure; and (3) Agricultural management and hydro-climatological controls will generate a cumulative critical control over DOC export dynamics, as runoff energy derived from a storm can be attenuated or strengthened by crop coverage at different growing stages.

2. Materials and methods

2.1. Study sites

The 270-km^2 Clear Creek Watershed (CCW), hydrologic unit code (HUC-10: 0708020901), is located in southeastern Iowa, USA. The Clear Creek flows from west to east as a tributary that drains the CCW into the Iowa River and eventually to the Mississippi River (Fig. 1a). The regional climate is humid-continental with a mean annual temperature of 9 °C, and abundant freeze-thaw cycles in early spring and late fall. The mean annual precipitation is 889 mm/year, with approximately 70 % of annual

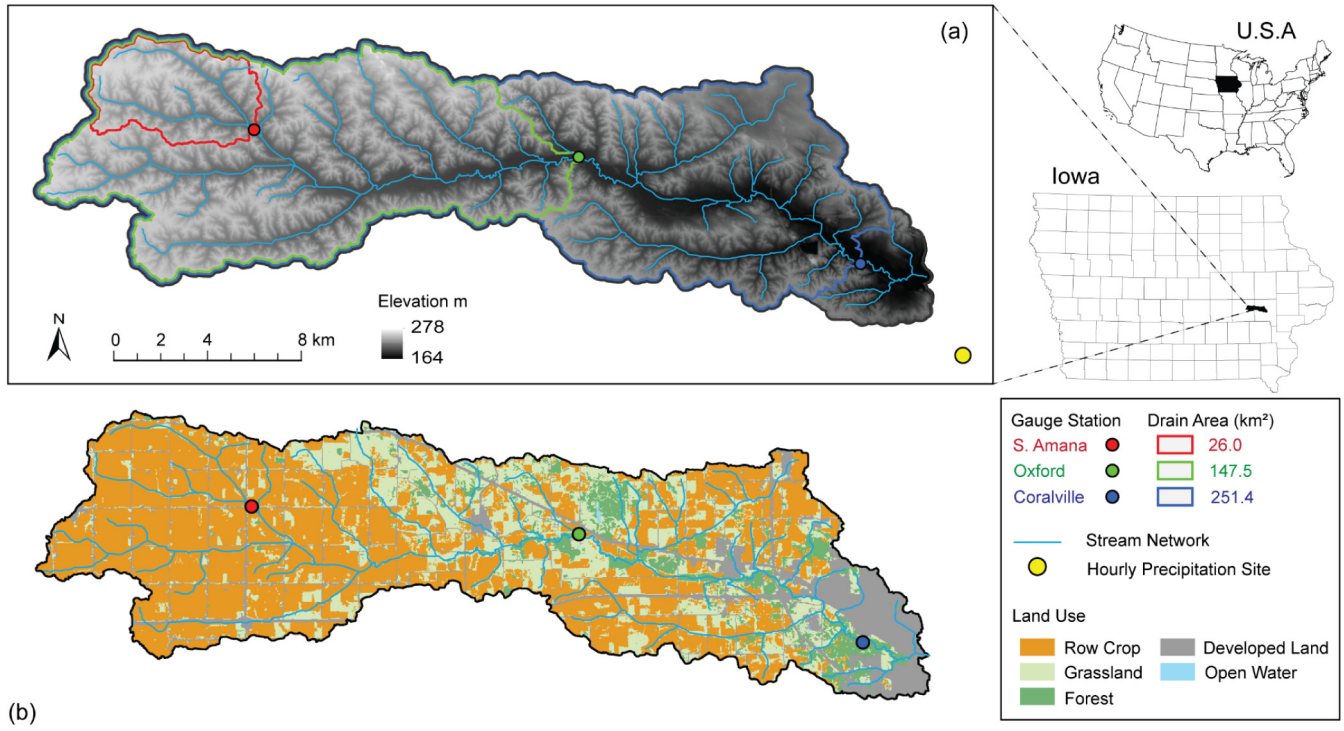

Fig. 1. (a) Elevation map of Clear Creek Watershed (CCW) showing drainage area of three stream gauge stations, stream network, and hourly precipitation site (yellow dot at southeast of the CCW); and (b) land cover of the CCW in 2015 derived from USDA/NASS Cropland Data Layer (https://www.nass.usda.gov/Research_and_Science/Cropland/SARS1a.php). (For interpretation of the references to colour in this figure legend, the reader is referred to the web version of this article.)

precipitation falling as rain during the months of May to September (the growing season) (Papanicolaou et al., 2009). During this wet period, heavy convective storms are capable of producing peak floods with significant hillslope erosion and sediment discharge into streams as a result of intensive tillage and stream channelization in the headwaters (e.g., Abaci and Papanicolaou, 2009; Wilson et al., 2018).

The CCW landscape is characterized as steep rolling, loess mantled hills with most of the soils being silty clay loam, silt loam, or clay loam Mollisols or Alfisols (Prior, 1991). Elevations range from 164 to 278 m above sea level with average slopes ranging from 6 % to 14 % at uplands. Over 80 % of the CCW is in some form of agricultural management (Bettis et al., 2003), predominantly cultivated crops (corn-soybean rotations) with combinations of conservation and conventional tillage. The normal timeline of row crop management is spring tillage/planting in early May, and harvesting/fall tillage in October (Abaci and Papanicolaou, 2009).

As part of the National Science Foundation Intensively Managed Landscapes - Critical Zone Observatory (IML-CZO), the CCW has been recently studied to assess how storm events control the delivery of soil, plant matter, and stream sediment and POC to the streams (Wilson et al., 2012; Papanicolaou et al., 2015a, 2015b; Abban et al., 2016; Blair et al., 2021; Hou et al., 2021). Additionally, over the last 140 years, like much of the floodplains and poorly drained soils in the upper Midwest of the US, an integrated network of belowground drainage tiles has been installed that hastens the delivery of the precipitation and the shallow groundwater to the streams (Schilling et al., 2018).

2.2. Storm event selection, gauge stations, and DOC sampling

During a two-hydrological year period (September 2014–August 2016), six storms were chosen from the nine events monitored in Blair et al. (2021) (Fig. 2). The six storms represented the most successful efforts to collect samples throughout the events at multiple stations within the drainage network. These six storms were small to intermediate in size and relatively short in duration. Small to intermediate-sized and short term events accounted for 82.9 % of the precipitation and 90 % of the storm duration (~2 day each) during the monitored period (Fig. A1). The sampled events occurred during periods of harvest, crop emergence, vegetative growth stage (Vn), reproduction growth stages of R1 and R2, and post-harvest/fall tillage (https://www.nass.usda.gov/Statistics_by_State/Iowa/Publications/Crop_Progress_&_Condition/).

The gauge and sampling station in the headwaters of CCW was located near South Amana (41°43′50″N, 91°54′26″W) and it captured drainage from a basin area of 26.0 km^2. It has been in operation since 2006 (Wilson et al., 2018). Land use there is mostly row-crop agriculture (Fig. 1b, Table 1). There is significant hydrologic connectivity between hillslopes and receiving channels, as a result of steep reach slopes (~6 %), narrow riparian zones, and agricultural practices (Abaci and Papanicolaou, 2009). The sampling stations at the middle and lower reaches were located proximal to the active U.S. Geological Survey (USGS) gauge stations; one near Oxford (USGS 05454220, in operation since 1993) and other near Coralville (USGS 05454300, in operation since 1952). The sampled drainage areas were 147.5 km^2 and 251.4 km^2, respectively. The middle-reach zone, while dominated by row crops, has increasing amounts of forest and grassland, especially along riparian zones (Fig. 1b; Abban et al., 2016). The lower reach of the CCW, while still agricultural, is proportionately the most developed with urban areas, and though it is a low-relief landscape, impervious surfaces accelerate runoff and flashiness (Fig. 1b; Papanicolaou et al., 2018). Channels are wider and deeper moving downstream, and valley cross-sections shifts from V-shape at headwater, to U- and box-shape at middle and lower reaches (Blair et al., 2021).

Stream stages and discharges were monitored at all three sites every 15 min along the main channel of the Clear Creek. Data at the S. Amana site were obtained from Blair et al. (2021) and those of the Oxford and Coralville sites were retrieved from USGS website (http://nwis.waterdata.usgs.gov) (Fig. 2b). Hydroclimatic characteristics during each event at different sampling stations were summarized in Table 2.

Stream waters were sampled—for POC (Blair et al., 2021) and filtered for DOC which the present study is based—shortly before, during, and on the tail of the storm events (Fig. 2), with frequency that varied from one sample every 2 to 4 h, depending on discharge variations. We attempted

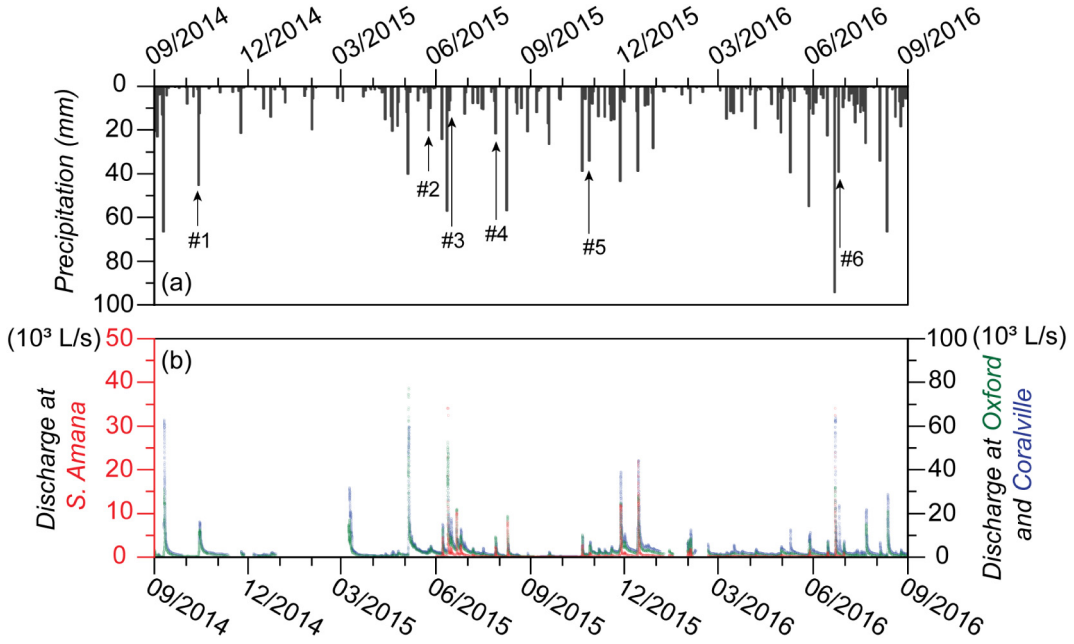

Fig. 2. Long-term monitoring of a) daily precipitation near Iowa City (retrieved from the NOAA National Centers for Environmental Information https://www.ncdc.noaa.gov/cdo-web/search?datasetid=GHCND); and b) 15-min discharges at three stations at S. Amana (red), Oxford (green) and Coralville (blue) in 10^3 *L/s* in the CCW. Black arrows and numbers denote the individual event selected in present study. (For interpretation of the references to colour in this figure legend, the reader is referred to the web version of this article.)

to complete the data set for both DOC and POC in the hydrograph across all three stream discharge sites covering all six storm events (Table A1). All water samples were collected in pre-rinsed 1-L Nalgene polycarbonate bottles equipped within the ISCO autosamplers (Teledyne ISCO, 6712 Portable Sampler), and transported to the laboratory to be frozen until processing. The ~800 mL thawed samples were filtered through roasted 0.7 μm pore size glass fiber filters (Millipore Sigma, Darmstadt, Germany). The filtered water was split into subsamples and placed in Nalgene bottles. Those for DOC were refrozen at −20 °C and stored in the freezer until analysis. Samples were kept in the dark to the extent possible. Freezing as a pre-analysis preservation strategy has been assessed for influence on DOC concentration with equivocal results with findings—suggesting an increase (Peacock et al., 2015), decrease (Fellman et al., 2008), and no difference (Rochelle-Newall et al., 2014). Though we recognize that water samples with high DOC concentrations (> 5 mg *C/L*) could be affected by aggregation, freezing was still the best preservation method for preserving the integrity of the chemical composition (Fellman et al., 2008).

2.3. DOC concentration analysis

DOC concentrations of filtered stream samples were determined using a high temperature combustion total organic carbon analyzer (Thermalox; Analytical Sciences Ltd., Cambridge, UK). Prior to analysis, 2 M HCl was added to the samples and purged to remove dissolved inorganic carbon. Potassium hydrogen phthalate (KHP; Inorganic Ventures, VA, USA) was used as the calibration standard (long-term R^2 = 0.9998). Four replicated measurements were taken for each sample, with a target coefficient of variation (CV) of 3 %. One additional replicate was added if the target CV was not achieved. Approximately, 10 % of samples were repeated in a separate run and those are reported with a mean value in the Results section. The maximum CV within a sample run and among different runs were 6.4 % and 11.9 %, respectively.

Table 1
Land use coverage (km^2) and relative contribution in % of S. Amana, Oxford, and Coralville drain areas (data was retrieved Cropland Data Layer (CDL) for year 2015 from the USDA CropScape Website https://nassgeodata.gmu.edu/CropScape/).

Land use km^2 (%)	S. Amana	Oxford	Coralville
Row crop	21.8 *(85)*	101.4 *(70)*	145.1 *(60)*
Grassland	2.2 *(7)*	30.7 *(20)*	59.9 *(23)*
Forest	0.2 *(1)*	4.0 *(2)*	17.5 *(6)*
Developed	1.7 *(7)*	11.0 *(8)*	27.8 *(11)*

Italic number in parentheses is proportion land use of row crop, grassland, forest and urban use in %, corresponding within each sub-watershed.

2.4. Fluvial OC export and hydro-climatological indices

Event-based OC export with respect to particulate (POC) and dissolved (DOC) forms, were estimated following (Blair et al., 2021),

$$Water\ yield\ (V, m^3) = \Sigma_i \frac{(Q_i + Q_{i-1})}{2} \times (t_i - t_{i-1}) \quad (1)$$

$$Event\ OC\ export\ (kg) = V \times \frac{\Sigma_i^n (C_i \times Q_i)}{\Sigma_i^n Q_i} \quad (2)$$

where V was calculated by integrating the 15-min discharge data over the event period, Q_i is discharge (*L/s*), C_i is DOC and/or POC concentration (*mg C/L*) of the instantaneous sampling point at time (t_i), and n is the number of samples. An early flush of DOC and/or POC was determined only if a prominent OC concentration peak appeared on the rising limb of the hydrograph within less than the 50th percentile of peak discharge (Table 2). Note that POC data were retrieved from the supplementary material in Blair et al. (2021).

Several normalizations were used to allow fair comparisons among multiple sites and various storm magnitudes. Concentration-discharge (C-Q) trajectories were normalized based on (Lloyd et al., 2016).

$$C_{i,norm} = \frac{C_i - C_{min}}{C_{max} - C_{min}}, and\ Q_{i,norm} = \frac{Q_i - Q_{min}}{Q_{max} - Q_{min}} \quad (3)$$

where Q_i is discharge and C_i is DOC and/or POC concentrations at time *i*; Q_{max} and Q_{min}, and C_{max} and C_{min} are the maximum and minimum discharge and DOC and/or POC concentrations (*mg C/L*) during the storm, respectively. Specific event export for DOC and POC ($kg\ C\ km^{-2}\ mm^{-1}$) was

Table 2
Comparison of storm characteristics for the six storm events across three sub-watersheds in terms of total precipitation during event (P_t), hydrograph duration (D_h), antecedent precipitation (AP_{30}), runoff coefficient (RC), unit stream power (SP), Flashiness Index (FI) and event integrated export of dissolved (DOC), particulate (POC), and early flush OC proportion (%).

		P_t (mm)	D_h (h)	AP_{30} (mm)	RC	SP (W/m)	FI	Integrated OC export (kg)[a]		% Early flush OC[b]	
								POC	DOC	POC	DOC
S. Amana	#2 (Jun. 2015)	35.1	40	72.4	0.18	180	0.038	NA	478	NA	NA
	#3 (Jun. 2015)	35.8	40	214.2	0.51	405	0.036	NA	1655	NA	NA
	#5 (Oct. 2015)	36.4	52	41.2	0.13	39	0.009	714	528 (43 %)	11.3	11.5
	#6 (Jun. 2016)	24.9	28	111.7	0.04	13	0.009	95	45 (32 %)	NA	NA
Oxford	#1 (Oct. 2014)	66.1	112	20.9	0.24	263	0.009	22,074	12,488 (36 %)	3.4	27.0
	#2 (Jun. 2015)	30.5	40	69.7	0.16	271	0.020	NA	3218	NA	NA
	#3 (Jun. 2015)	29.6	40	191.4	0.33	459	0.020	NA	5738	NA	NA
	#4 (Jul. 2015)	45.5	32	73.4	0.08	195	0.026	14,397	2083 (13 %)	2.6	3.0
	#5 (Oct. 2015)	36.2	52	46.0	0.14	125	0.009	6203	3894 (39 %)	4.4	4.0
	#6 (Jun. 2016)	25.4	26	127.6	0.04	42	0.007	780	407 (34 %)	NA	NA
Coralville	#4 (Jul. 2015)	39.2	30	67.3	0.05	148	0.029	11,967	2054 (15 %)	NA	NA
	#5 (Oct. 2015)	36.1	54	49.4	0.10	121	0.009	5273	4137 (44 %)	3.1	3.3
	#6 (Jun. 2016)	30.0	26	157.3	0.11	396	0.042	34,290	2331 (6 %)	NA	NA

[a] POC data was extracted from Blair et al., 2021. Proportion (%) of DOC over total OC export was reported in parentheses. NA (not available) means there was not enough data points to calculate POC export and/or no early flush of POC/DOC during specific events.
[b] If there is a peak of OC concentration at the early stage of rising limb on hydrograph, the early flush OC was identified and quantified as % of total event OC export.

calculated by dividing the absolute OC export (*kg*) by the sub-watershed sizes (km^2) and precipitations (P_t in *mm*). Flow weighted mean concentrations for DOC and POC ($FWMC_{DOC}$ and $FWMC_{POC}$, *mg C/L*) was calculated by dividing the event-based OC export (*kg*) by the total water yield (m^3).

To quantify hydro-climatological characteristics of each storm, a database containing critical indices was selected and calculated for each storm event within each sub-watershed (i.e., S. Amana, Oxford, and Coralville) (Table 2). Specifically, runoff coefficient (*RC*) was calculated by dividing total yield stormflow (*mm*) by the total precipitation (*mm*), indicating a watershed's draining capability when receiving waters (Blume et al., 2007). Unit stream power (*SP*) was adjusted from Bagnold (1966) equation,

$$SP = \rho \cdot g \cdot Q \cdot S \quad (4)$$

where *SP* is stream power per unit of flow length (*W/m*); ρ is water density (kg/m^3); *g* is gravitational acceleration (m/s^2); *Q* is the peak discharge during the period of storm event in this study (Q_{max}, m^3/s); and *S* is local channel slope (*m/m*). *SP* is widely used in sediment studies as an indicator of energy supply for functional transport, with consideration of both hydrology (i.e., discharge) and waterway geomorphology (i.e., channel slope) (De Rosa et al., 2019).

Richards-Baker Flashiness Index (*FI*) was adopted based on Baker et al. (2004),

$$FI = \frac{\sum_i^n |q_i - q_{i-1}|}{\sum_i^n q_i} \quad (5)$$

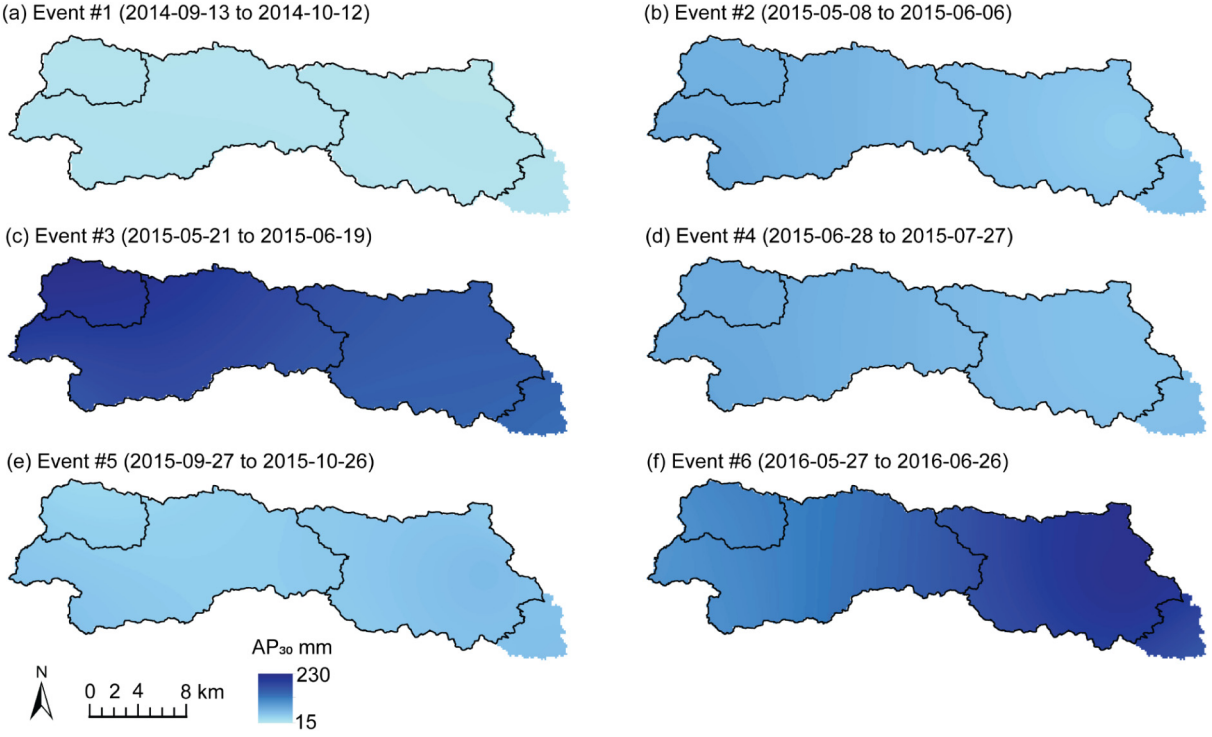

Fig. 3. Maps showing the spatial interpolation on the antecedent precipitation in the 30 days prior to the event day (AP_{30}) for storm events #1-#6 (a-f). Legend shows the cumulated precipitation in mm, with the black outline on the maps highlighting each sub-watershed drainage area in the CCW, which was used for area weighted mean value calculations. Data was retrieved from the NOAA National Centers for Environmental Information (https://www.ncdc.noaa.gov/cdo-web/search?datasetid=GHCND).

The *FI* parameter measures "flashiness" in flow change relative to the total hydrograph, reflecting the rapidity of difference between high and low flows. Additionally, event precipitation (P_t, *mm*), hydrograph duration (D_h, *h*), peak stream discharge (Q_{max}, *L/s*), and antecedent precipitations (*AP*, *mm*) were also reported for each event (Table 2, and Table A2). Antecedent precipitations (AP_3, AP_7, AP_{14} and AP_{30}) were cumulative precipitation of 3, 7, 14, and 30 days prior to event day.

2.5. Spatial precipitation estimation

Hourly precipitation data was only available at Iowa City (6-km southeast of the Coralville outlet of CCW, yellow dot in Fig. 1a) through the Iowa Environmental Mesonet (http://mesonet.agron.iastate.edu). To compare storm event precipitation distributions across three sub-watersheds in the CCW, given the lack of hourly data at the headwaters (S. Amana) and the mid-reach (Oxford), the daily precipitation data of nine USGS rain gauge stations surrounding the CCW were retrieved from the NOAA National Centers for Environmental Information (https://www.ncdc.noaa.gov/cdo-web/search?datasetid=GHCND) (Fig. A2). Daily precipitation and antecedent cumulated precipitation distribution data were then spatially interpolated using the inverse distance weighting (IDW) method (Garcia et al., 2008). Interpolation and generation of spatial maps shown in Fig. 3 (e.g., antecedent precipitations of 30 days prior to event day, AP_{30}), were performed in Arc GIS 10.7.1 software, where mean estimated precipitation (*mm*) for individual events across three sites were quantified upon sub-watershed areas (Tables 2 and A2).

2.6. Land cover and NDVI data

Spatial land coverage in CCW was characterized using the Cropland Data Layer (CDL) for the year 2015 from the USDA CropScape Website (https://nassgeodata.gmu.edu/CropScape/) (Boryan et al., 2011), which provides a geo-referenced, crop-specific land cover map for the U.S. since 1997. The CDL was downloaded and reclassified as row crop land, grassland, forest, open water areas, and developed urban areas (Fig. 1b). The proportions of different land use coverage were then delineated and quantified based on sub-watershed area for each site (i.e., S. Amana, Oxford, and Coralville) in ArcGIS 10.7.1 software (Table 1).

NDVI (Normalized Difference Vegetation Index) is calculated as a ratio between the red (R) and near-infrared (NIR) values with the formula (NIR - R) / (NIR + R), derived from atmospherically corrected land surface reflectance; this results in a value between 0 and 1. The NDVI has been proven to improve the sensitivity of assessing vegetation conditions, where higher values associated with denser vegetation (> 0.80 for well-vegetated forests), and more sparse vegetation and/or exposed bare soil surface are associated with lower values (< 0.30) (Yang et al., 2013). As a vegetation index, NDVI has been reported to be closely related to surface coverage and aboveground productivity (Carlson and Ripley, 1997) to assess land degradation (Yengoh et al., 2015; Ren et al., 2020). Additionally, the NDVI has been used to link vegetation productivity to DOC concentration in lakes and water reservoirs (Larsen et al., 2011a, 2011b; Mzobe et al., 2018). A weekly NDVI map spanning the time immediately before each monitored storm event was extracted from the USDA National Agricultural Statistics Service Vegetation Condition Explorer (https://nassgeo.csiss.gmu.edu/VegScape/) (Fig. 4), imported in Arc GIS 10.7.1 software, and delineated based on sub-watershed areas.

2.7. Statistical analyses

A Pearson correlation matrix showing coefficients with significance levels (Table 3), was generated to compare the relationship between

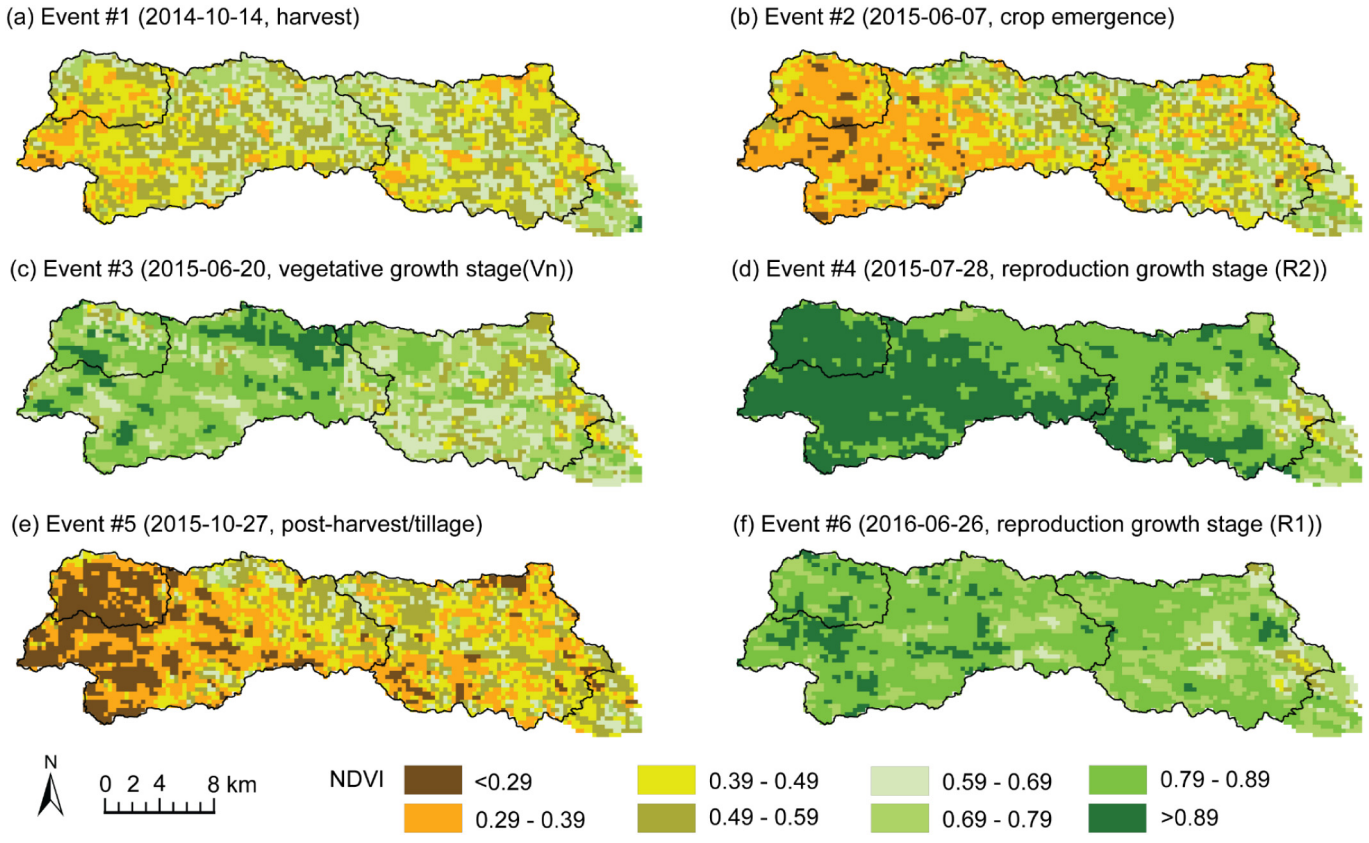

Fig. 4. Weekly Normalized Difference Vegetation Index (NDVI) maps during or before the storm events #1- #6 (a-f). Event date and corresponding periods of planting and growing at that time derived from Iowa Crop Progress and Condition Report are given in parentheses. Raster maps were extracted from USDA National Agricultural Statistics Service Vegetation Condition Explorer (https://nassgeo.csiss.gmu.edu/VegScape/). Black outline on the maps highlights each sub-watershed drainage area in the CCW, which was used for area weighted mean value calculations.

Table 3
Pearson Correlation matrix among selected hydroclimatic variables and flow-weighted mean concentration (FWMC), event integrated export (EXP) of DOC and POC, and export ratio of POC:DOC.

	P_t	RC	SP	FI	AP_{30}	NDVI	$FWMC_{DOC}$	EXP_{DOC}	$FWMC_{POC}$	EXP_{POC}	POC:DOC
P_t	1										
RC	0.18	1									
SP	0.11	**0.73****	1								
FI	−0.09	0.33	**0.61***	1							
AP_{30}	−0.51	0.55	**0.61***	0.47	1						
NDVI	−0.18	−0.02	0.25	0.30	**0.61***	1					
$FWMC_{DOC}$	**0.63***	0.20	0.10	−0.31	−0.54	−0.55	1				
EXP_{DOC}	0.36	**0.96*****	**0.69****	0.14	0.36	−0.14	0.43	1			
$FWMC_{POC}$	0.04	−0.08	**0.78***	**0.95*****	0.46	0.53	−0.14	−0.20	1		
EXP_{POC}	0.28	0.39	**0.97*****	**0.80****	0.30	0.22	0.04	0.23	**0.84****	1	
POC:DOC	−0.13	−0.11	**0.79***	**0.96*****	0.64	0.53	−0.34	−0.28	**0.94*****	**0.87****	1

Correlation coefficients notes in bold with significant p-values at * $p < 0.05$; ** $p < 0.01$; and *** $p < 0.001$.
See Materials and method section for variable description.
$n = 9$ for correlation including POC, otherwise $n = 13$.
POC data was extracted from Blair et al., 2021.

selected hydroclimatic and watershed variables to event DOC and/or POC concentrations, and OC export for all six events. Agglomerative hierarchical clustering with Ward's method employed, was used to group all the events into two clusters based upon selected hydro-climatological variables (i.e., sub-watershed NDVI and 30-day antecedent precipitation). Events within each cluster are coherent internally but distinctly different between clusters. Pearson correlation analysis was then conducted for cluster 2 (Fig. 6) between selected hydro-climatological variables and DOC export with significance at the 95 % confidence interval. Because of non-normality of DOC export in cluster 1 (right-skewed distribution), Spearman rank correlation was carried out with Bonferroni correction for *P* values adjustment. All statistical analyses were performed with the R Studio program (Version 2022.7.1.554, R Core Team, Inc., Boston, MA).

3. Results

3.1. Event integrated DOC versus POC export

Overall, DOC export integrated for individual events increased from headwater to middle and lower reaches, with ranges of 45–1655 kg, 407–12,488 kg, and 2331–4137 kg observed at S. Amana, Oxford, and Coralville station, respectively (Table 2). Combined with POC export reported in Blair et al. (2021), DOC accounted for only 6–44 % of total fluvial OC export (Table 2), and the differences were tied to key hydrologic indices, i.e., runoff coefficient and stream power (Fig. 5). Specifically, POC export was strongly correlated with the stream power (*SP*, $r = 0.97$; $p < 0.001$; Fig. 5d), an index of sediment transport (De Rosa et al., 2019). Similarly, DOC exhibited a strong correlation between the export and the runoff coefficient (*RC*, $r = 0.96$; $p < 0.001$; Fig. 5c), an index of draining capability (Blume et al., 2007). Conversely, the *SP* – DOC export and the *RC* – POC export correlations were weak (Table 3, Fig. A.3). Accordingly, POC:DOC export ratios did not consistently correlate with either index. Hydrographic 'flashiness' (*FI*) was strongly correlated with POC associated parameters (Table 3).

3.2. Management and hydrological controls on clustered DOC exports

We hypothesized that two indices, weekly NDVI and AP_{30}, would influence DOC export (Fig. 6a and b). Linear relationships were not evident when all data are considered within a single group. Visual inspection of the data (Fig. 6 a, b), and unsupervised hierarchical clustering (Fig. 6c) revealed two groups of data however, of the two clusters, only one (cluster 2) exhibited significant correlations, where DOC export responded negatively to NDVI and positively to AP_{30} ($p < 0.05$, Fig. 6d). No significant correlations were found in cluster 1. Cluster 2 was best characterized as having a near uniform and relatively high vegetation cover, as well as higher AP_{30} values.

3.3. Temporal variation of OC concentration and C-Q hysteresis patterns

The temporal variability of the DOC and POC concentrations behaved differently among the six storm events across three sampling stations in CCW (Figs. 7, 8, A4 and A5). For events #3, #4, and #6, which were captured during the rapid growing season (i.e., cluster 2), in June/July, there was a tendency for a lagged DOC peak concentration following peak discharge and peak POC concentration (Figs. 8 and A5). Events #1 and #5 occurred post-harvest in late October (i.e., cluster 1), when agricultural fields contained fresh crop residue and bare surface soil (Iowa Field Office). They showed significant positive correlations between DOC and POC concentration (Figs. 7 and A4). The differential responses of DOC and POC across the entire CCW reflected several general patterns of 1) greater concentration difference between POC and DOC at the middle (Oxford) and lower (Coralville) reaches of the watershed compared to the headwaters (S. Amana), and 2) greater difference between POC and DOC during the June/July events (event #4 and #6) compared to the October events (event #1 and #5).

DOC concentration (*C*) to discharge (*Q*) relationships (C_{DOC}-*Q*) exhibited both clockwise and counterclockwise hysteresis patterns in contrast to C_{POC}-*Q* relationships that typically shown clockwise patterns for all the events (Figs. 7, 8, A4 and A5). Specifically, the C_{DOC}-*Q* relationship exhibited a clockwise pattern for October events #1, and #5 (Figs. 7 and A4), while counterclockwise C_{DOC}-*Q* trajectories were observed in June/July events #3, #4 and #6 (Figs. 8 and A5). One exception is event #2 in early June 2015 which demonstrated clockwise C_{DOC}-*Q* relationship like the reported October events (Fig. A4 d and f). Based on the Iowa Crop Progress and Condition Report, crops were at the early stage of seed emergence during the week of event #2, though in the wet growing season of early June, where land was still bare, with limited surface coverage. Unsupervised hierarchical clustering grouped this event with other October events in the same cluster (i.e., cluster 1, Fig. 6c).

4. Discussion

4.1. Storm-induced POC export consistently exceeds DOC export

In contrast to the present work, numerous studies on OC export have reported greater contributions of DOC over POC, however, these estimates normally were extrapolated from surface water fluvial OC concentrations derived from periodic/non-event based sampling (e.g., Hedges et al., 1997; Cai et al., 2008; Alvarez-Cobelas et al., 2012; Fabre et al., 2019; Mu et al., 2019). In a review of worldwide annual OC export, Alvarez-Cobelas

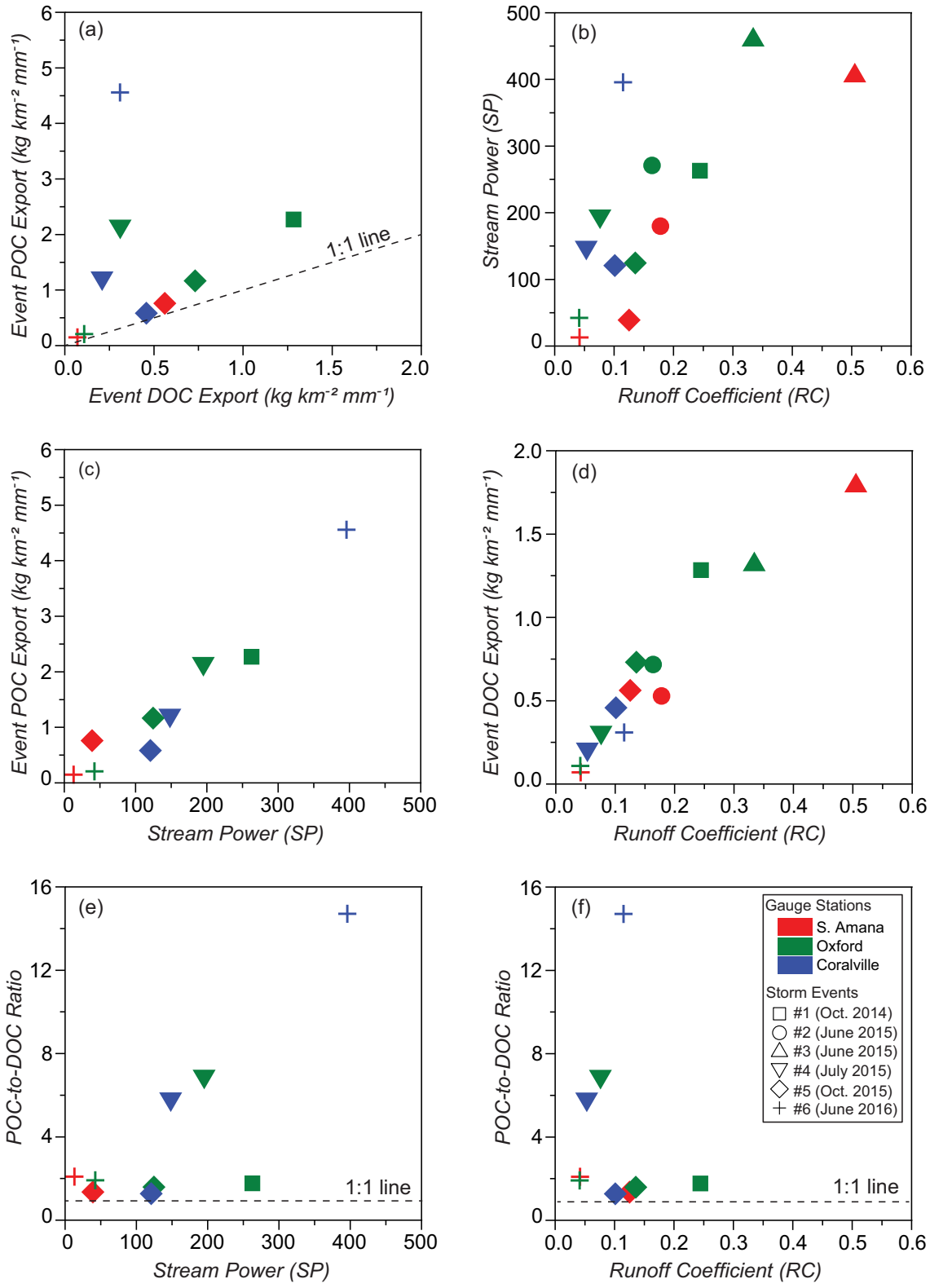

Fig. 5. Comparison of (a) event export of DOC to POC, (b) runoff coefficient (RC) to stream power (SP), (c) SP to POC export, (d) RC to DOC export, (e) SP and (f) RC to POC-to-DOC ratio among events #1 (square), #2 (circle), #3 (up-triangle), #4 (down-triangle), #5 (diamond), and #6 (crisscross) at S. Amana (red), Oxford (green) and Coralville (blue) sites. 1:1 line was plotted with dotted lines. (For interpretation of the references to colour in this figure legend, the reader is referred to the web version of this article.)

et al. (2012) estimated that DOC was 73 ± 21 % of total OC exports from catchments across a wide range of sizes, land uses, soil types, and locations. However, and similar to our findings, some recent studies based on a high-resolution sampling strategy designed to capture OC exports during high-flow periods have proposed a chronic underestimation of POC (e.g., Oeurng et al., 2011; Jeong et al., 2012; Dhillon and Inamdar, 2014). We found that event-induced OC export exhibited a consistently greater dominance of POC compared to DOC, across multiple storm events,

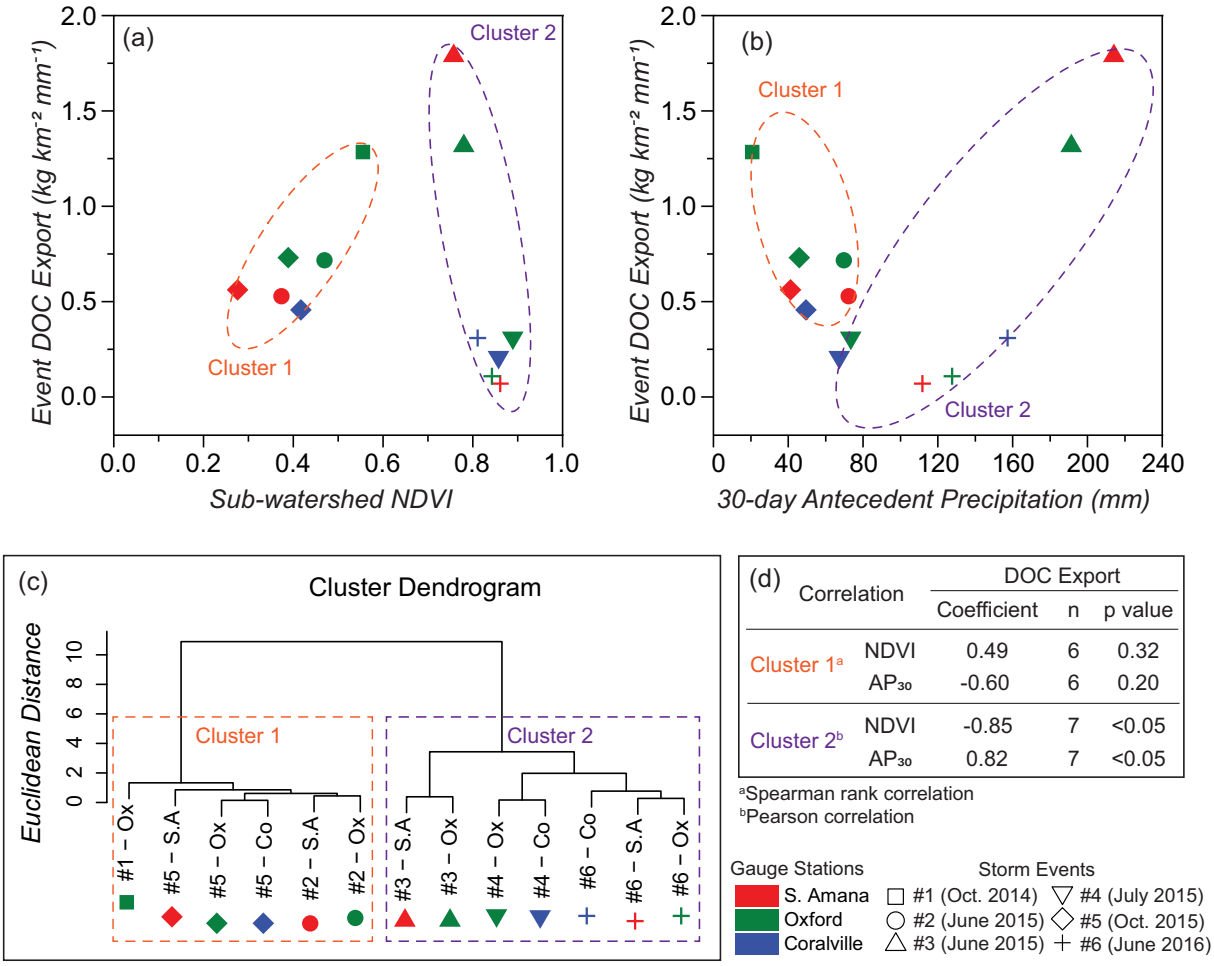

Fig. 6. Comparison of DOC export with (a) sub-watershed NDVI, and (b) 30-day antecedent precipitation among events #1 (square), #2 (circle), #3 (up-triangle), #4 (down-triangle), #5 (diamond), and #6 (crisscross) at S. Amana (red), Oxford (green) and Coralville (blue) sites. Hierarchical clustering results shown two distinct clusters outlined in orange and purple (c), with correlation coefficients and *p*-values analyzed within each cluster (d). (For interpretation of the references to colour in this figure legend, the reader is referred to the web version of this article.)

where the export ratio of POC:DOC ranged between 1.3 and 14.7 (Table 2). To generalize the POC and DOC export pattern beyond our limited data sets, we compiled fluvial OC export data reported in published studies monitoring both DOC and POC during high-flow conditions (Oeurng et al., 2011; Jeong et al., 2012; Caverly et al., 2013; Cerro et al., 2014; Dhillon and Inamdar, 2014; Ramos et al., 2015). These six studies included detailed event characteristics and integrated export for both DOC and POC, and so the OC exports can be normalized based on precipitation and drainage area and be directly compared with our own findings. The export ratios of POC:DOC from the high-resolution sampling studies ranged between 0.1 and 14.7, with over 81 % of events ($n = 69$) exhibiting a POC:DOC export ratio above 1.

To highlight how sampling strategy can control OC export dynamics in our work, we created a theoretical sampling calculation comparison with one scheme sampling baseflow only and another sampling scheme capturing both baseflow and storm flow, where we then estimate monthly POC and DOC exports in October and June at the Oxford station between 2014 and 2016. The resulting non-event based estimations from this exercise consistently showed POC export being under-evaluated monthly, by a factor of 1.9–5.4 fold. A non-event based sampling resulted in a clear sampling bias with POC:DOC export ratio of 0.5–1.5, as compared to a POC:DOC export ratio of 1.4–4.2 where storm-flow OC was included. These estimations demonstrate how event-driven dynamics favor POC over DOC export and that low-resolution and non-event based analysis of fluvial OC dynamics will under assess not only total OC export but the importance of POC as a proportion of total fluvial OC export.

Greater storm event response of POC over DOC can be explained, in large part, by the direct relationship between particulate transfer and surficial erosional processes triggered by hydraulic forcing (Battin et al., 2008). Using $\delta^{13}C$ and $\delta^{15}N$ isotopes of POC and particulate nitrogen (PN), Blair et al. (2021) demonstrated complex watershed-scale interactions controlling POC dynamics in CCW that were driven by sequential processes of surficial erosion as well as stream bed scouring associated with increasing precipitation and discharge. In that study, it was proposed that POC export tends to be intermittent and influenced by the locations of source areas, geomorphology, and obstruction along its pathway to the stream (Papanicolaou et al., 2015a, 2015b). Likewise, our evidence of a strong, positive correlation between POC export and unit stream power in CCW supports this conclusion (Fig. 5c). Compared to a weaker correlation between DOC export and unit stream power (Fig. A3b), POC export should thus be more sensitive to event-induced transferring flow with high hydrodynamic energy than DOC export.

In line with this erosion-driven mechanism, more prominent POC export would most likely occur if storms are selectively sampled with higher levels of hydrodynamic forces, i.e., stronger storms, that can promote upland soil and/or stream bank erosion (Blair et al., 2021). On the other hand, DOC export responding to stronger storms might be distinguishable as an accretion or dilution effect, resulting in varying POC:DOC export

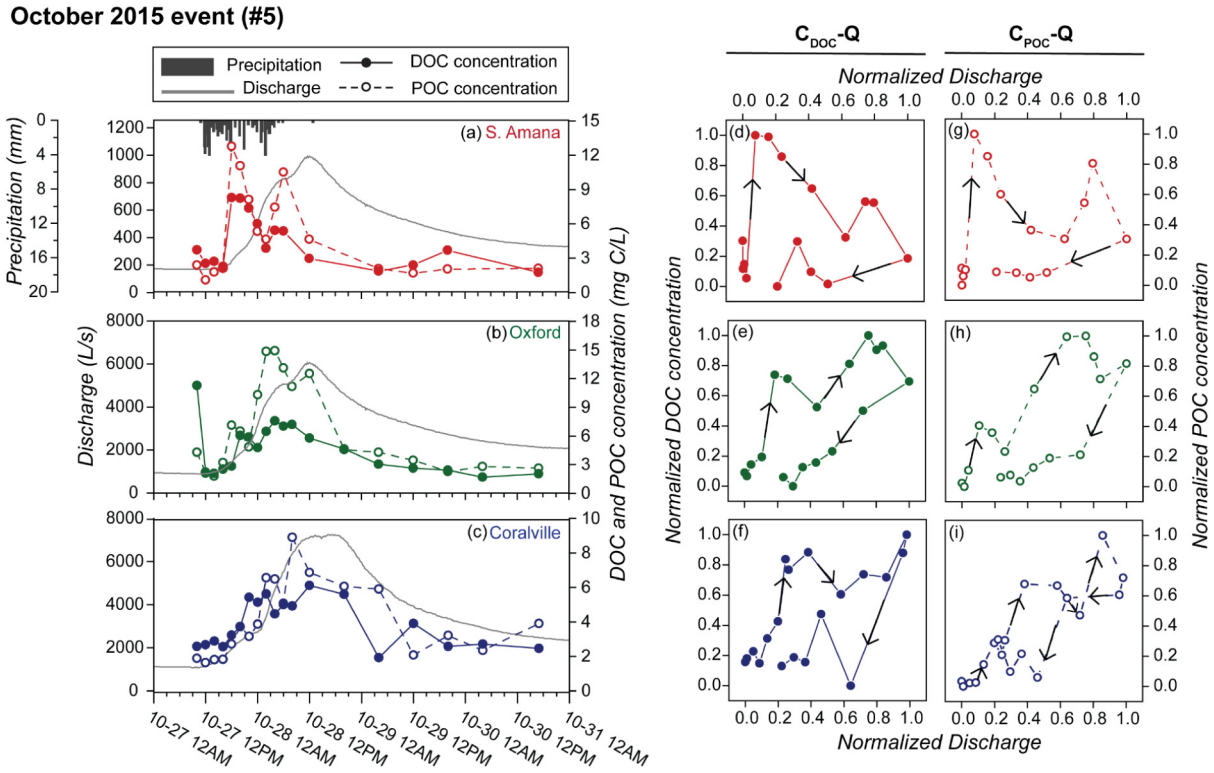

Fig. 7. Temporal variations of POC and DOC concentrations (mg *C/L*) over the discharge measured at three sampling stations (a), (b), and (c) for event #5 in October 2015; and normalized C-Q (DOC and POC concentration to discharge) relationships show hysteresis patterns across different stations ((d)-(i); arrows are shown the direction over time). Precipitation bars are hourly values reported at the station situated at southeast of the CCW. POC data was extracted from Blair et al., 2021.

ratios. That is, during a strong storm, more DOC pools can be activated with increased transfer energy, or this energy-induced influence can be outpaced by total event water input (Vaughan et al., 2017). During Hurricane Irene, Caverly et al. (2013) measured 1270 kg km^{-2} of DOC flux from an agricultural watershed in Virginia, USA. Also during Hurricane Irene, Dhillon and Inamdar (2014) reported a forested watershed in Maryland, USA exported 330 kg km^{-2} of DOC. With comparable rainfall, these two studies yielded differential POC:DOC export ratios of 0.5 and 6.7, respectively (circled points in Fig. 9). These observations suggest caution is needed when evaluating POC and DOC export relationships, particularly under future climate

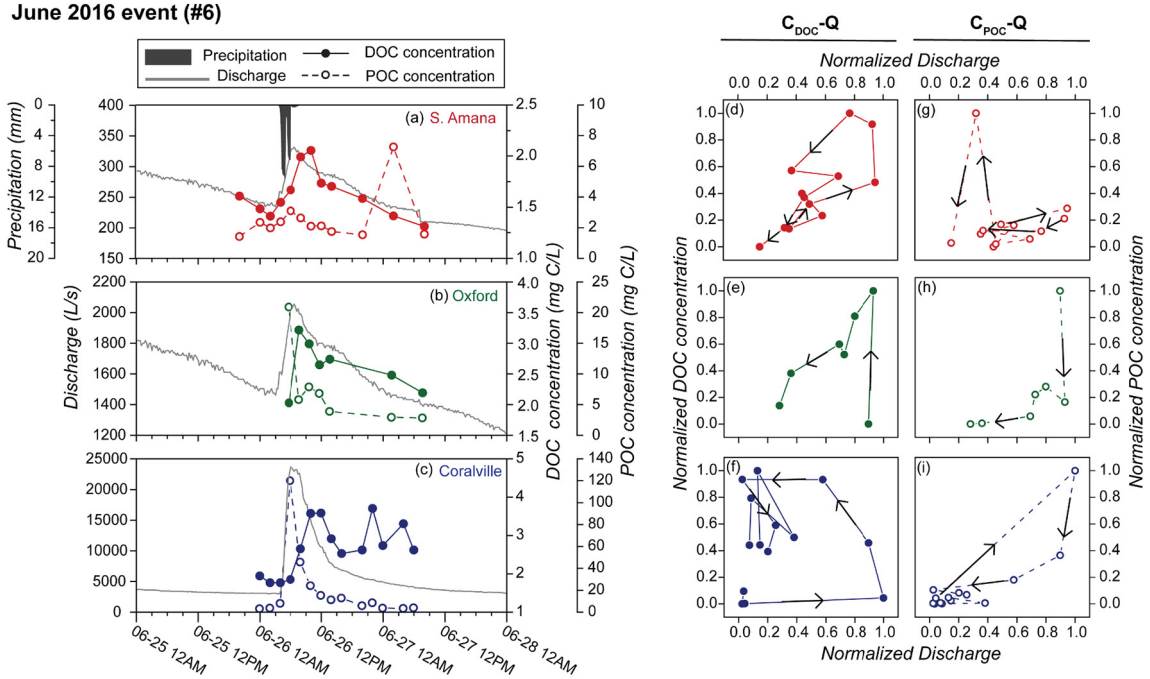

Fig. 8. Temporal variations of POC and DOC concentrations (mg *C/L*) over the discharge measured at three sampling stations (a), (b), and (c) for event #6 in June 2016; and normalized C-Q (DOC and POC concentration to discharge) relationships show hysteresis patterns across different stations ((d)-(i); arrows are shown the direction over time). Precipitation bars are hourly values reported at the station situated at southeast of the CCW. POC data was extracted from Blair et al., 2021.

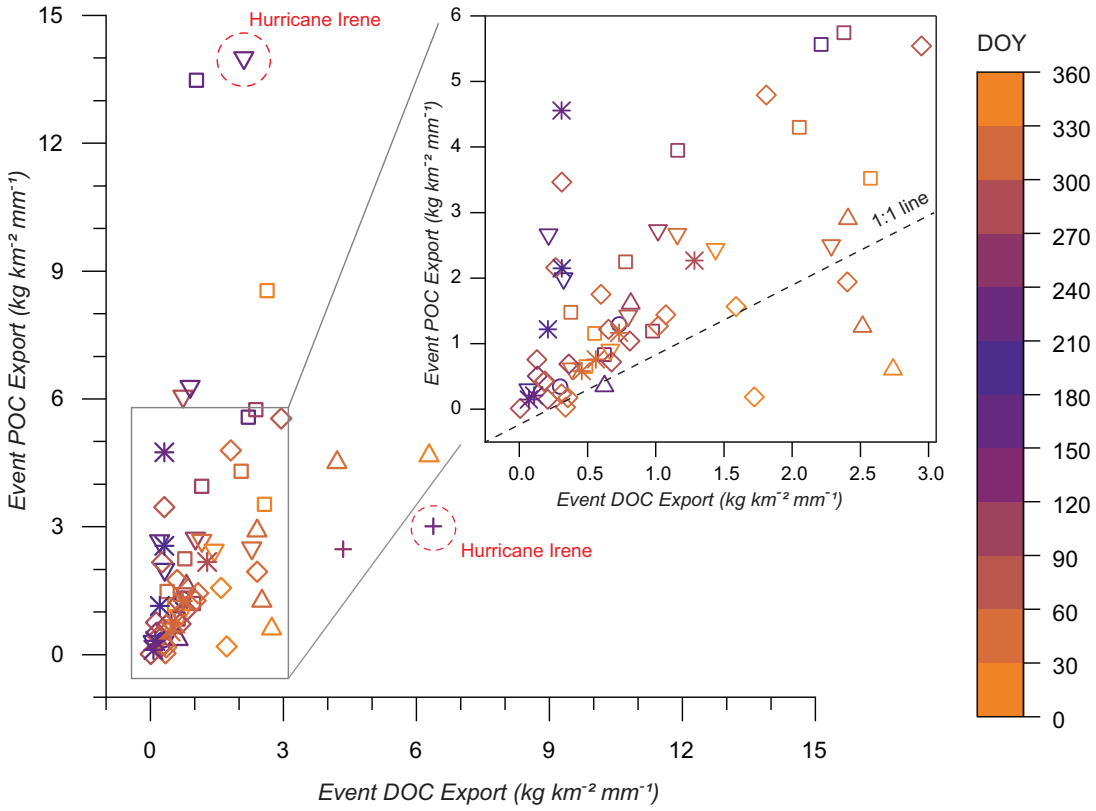

Reference	Location	Watershed size km²	No.of event	Land use
✳ Present Study	Iowa, USA	260	6	60% agriculture (corn and soybean)
□ Oeurng, 2011	Southwest France	1110	13	90% agriculture (sunflower and winter wheat)
○ Jeong, 2012	South Korea	60	2	Mixed coniferous and deciduous forest
△ Cerro, 2014	Northern Spain	53	7	75% agriculture (wheat, oat and barley)
▽ Dhillon, 2014	Maryland, USA	0.12	13	Mostly deciduous forest
◇ Ramos, 2015	Southern Portugal	61	23	Mostly olive groves, holm-oaks, and winter crops
+ Caverly, 2013	Virginia, USA	0.21	2	Mostly agriculture (corn, soy, and winter wheat)

Fig. 9. Comparison between storm induced DOC and POC exports per drainage area and event precipitation across variable references regarding land uses, locations, basin sizes and day of year (DOY, represented within the colour range), where different shaped icon extracted from references listed in the table. Two extreme events related to Hurricane Irene were outlined in dotted red circles. POC data used in present study was extracted from Blair et al., 2021. (For interpretation of the references to colour in this figure legend, the reader is referred to the web version of this article.)

change scenarios with expected increases in frequency and magnitude of drought and extreme events (Stanley et al., 2012).

4.2. Seasonal controls on event-driven POC and DOC export

During the two hydrological year period monitored in the present study, summer events (June/July) were generally associated with high-intensity rainfall and produced flashy/short-duration of stormflow hydrographs (Figs. 2 and 9). Besides producing flow with high hydrodynamic energy, summer events were also likely associated with abundant OC supply driven by warming and repeated drying-rewetting cycles. Elevated temperature and successive events in summer have been shown to enhance both above- and below-ground productivity, in-stream primary production (Baumann et al., 2013), and decomposition, dissolution, and desorption of soil organic matter (Raymond and Saiers, 2010). During summer June/July events of the present study, POC responded nearly instantaneously to rapid increase of discharge, and this resulted in a greater disparity, up to 32 times, between peak POC concentration and that of DOC as compared to events in late fall (Figs. 8 and A5). The lagged and attenuated DOC concentration peak observed suggests different thresholds of transport flow and/or OC supply for DOC and POC in summer events. This phenomenon of seasonal controls in relative POC/DOC export has been observed in a variety of landscapes including primarily forested systems (e.g. Dhillon and Inamdar, 2014) in which case high-intensity flow transport occurred during times of increased primary and secondary production in summer.

The CCW events from late fall (October) were less flashy and produced gradual/longer-duration flow hydrographs (Fig. 2). Integrating OC concentration over the entire hydrograph, revealed an event export ratio of POC: DOC that remained relatively low (1.3–1.7) even when the sediment transport associated flow parameters (i.e., the unit stream power and runoff coefficient) were increasing, which contrasted with the June/July events that yielded a much higher (up to a value of 14.7) POC:DOC export ratio (Fig. 5e and f). During these October events, smaller differences were observed between total POC and DOC export, and the POC and DOC dynamics were similar in the timing and magnitude of maximum concentrations (Figs. 7 and A4), further implying that a common OC source is activated and a common preferential pathway for delivering both OC forms.

4.3. Event-driven DOC export response to NDVI and antecedent wetness conditions

While event-driven export and peak concentration for DOC were always less than the corresponding POC values in both June/July and October events (Tables 2 and A2), the distinct DOC concentration dynamics among storms suggest a threshold control on OC supply and transport pathway that differ seasonally. Seasonality-based agricultural management in CCW generates potential sub-watershed differences in surface coverage and biotic productivity throughout the growth stages that influence surface erosion, below-ground water transfer, and overall OC export dynamics. The Normalized Difference Vegetation Index (NDVI) and antecedent precipitation (AP_{30}) for CCW were used as indices of vegetation coverage and antecedent wetness conditions in the present study to illustrate their controls over DOC export. Although the number of monitored events in the present study was few ($n = 6$), they fell into two general agricultural and hydroclimatic periods that are common in midwestern agricultural systems; the antecedently-dry, bare soil period (cluster 1, referred as the "bare soil" period below), and the antecedently-wet, rapid growth period (cluster 2, referred as the "rapid growth" period below, Fig. 6c).

Overall, the relationships between NDVI and AP_{30}, and event DOC export were non-linear (Fig. 6a and b) with significant correlations only observed in cluster 2 ("rapid growth" period) where event-driven DOC export responded negatively to NDVI and positively to AP_{30}. Although not significant, DOC from cluster 1 appears to exhibit a reversed (positive) relationship to NDVI and (negative) to AP_{30}. NDVI has been shown to exhibit a close linkage with OC export in freshwater systems, where higher NDVI values are thought to correspond to increased OC leachates from plant primary production (Larsen et al., 2011a, 2011b). With this perspective in mind, DOC pools available for events occurring within cluster 2 could be considered as "supply-abundant" OC, and thus any observed decreases in the amount of DOC delivered to the stream (Fig. 6a) would be a result of differences in transport flows (i.e., changes in runoff vs tile flow) not available at a source. Hence, event-driven DOC export with increased AP_{30} in cluster 2 (Fig. 6b) can be explained by a "wetter" watershed exhibiting a lower threshold of runoff generation that facilitates runoff-associated DOC export in response to rainfall (Cain et al., 2022). In contrast, low OC availability at a site, as inferred by low NDVI, could be a controlling factor for event-driven DOC export within cluster 1 (Fig. 6a). A potential explanation for the seemingly negative correlation between DOC export and AP_{30} in cluster 1 (Fig. 6b), could be that during the "bare soil" period, less surface coverage by crops enhances overland flow generation when receiving rainfall, and thus could potentially outpace the influence of antecedent wetness of watershed on runoff generation (Blair et al., 2021; Cain et al., 2022).

While we recognize the weak statistical power due to the limited data set, our analysis suggests that there may be a strong interaction or competing influences between the surface coverage of vegetation (as a surrogate for active production of terrestrial OC) and runoff-generation threshold controls by antecedent watershed wetness, which allows for the discrimination of the six storm events for three sub-watersheds, highlighting differential responses. The data from the CCW, considered from a management and hydroclimatic control perspective through NDVI and AP_{30} lens, indicates there are seasonal shifts in DOC source and transport pathway driven primarily by the degree of vegetation coverage/growth.

4.4. Intra-storm C_{DOC}-Q hysteresis reflects OC source and transport mechanisms

The relationship between concentration (C) of POC and DOC and discharge (Q) can provide key insights into the nature of delivery processes for fluvial OC (Vaughan et al., 2017; Liu et al., 2021). In the present study, POC displayed a consistent clockwise hysteresis for both clusters, while DOC revealed clockwise and counterclockwise patterns for events in cluster 1 and cluster 2, respectively (Figs. 1, 8, A4, and A5). Blair et al. (2021) attributed the clockwise C_{POC}-Q hysteresis in the CCW to the delivery of in-stream sources, easily erodible sediment, and stream bank sources during the rising limb of the hydrograph, and then these sources were exhausted and/or diluted later in the storm. A thorough examination of intra-storm DOC dynamics between events in two clusters helps explain different hysteresis patterns seen for C_{DOC}-Q. Here we chose October 2015 event (#5, Fig. 7) and June 2016 event (#6, Fig. 8) as representatives of cluster 1 ("bare soil" period) and cluster 2 ("rapid growth" period) contrasting times where dominant crops were post-harvest or in a reproduction growth stage (R1).

4.4.1. The "bare soil" period exhibits rapid liberation of DOC

During the October 2015 event, the three sub-watersheds (i.e., S. Amana, Oxford, and Coralville) all exhibited clockwise C_{DOC}-Q hysteresis, suggesting a DOC transport mechanism of rapid liberation from within- and near-to-stream sources and/or upland sources that are easily erodible in early stormflows (Blair et al., 2021). A pronounced early DOC pulse occurred during the very early stage of the rising limb and its mobilization was due to easy accessibility and erodibility (Fig. 7). Using stable carbon and nitrogen isotope analyses, Blair et al. (2021) identified the sources of accompanied POC pulse as a combination of leftover of corn and soybean residue mixed with upland agricultural soils. These easily erodible OC-rich sources were then exhausted or cut off as precipitation ceased. Following the 'early pulse', the main DOC peak that increased with increasing discharge subsided sharply before the peak discharge. Our finding of an early DOC pulse are in-keeping with others who similarly explain this C-Q relationship feature as dominated by rapid mobilization from hillslopes (Jeong et al., 2012), one where a proximal OC-rich sediment source near and/or within streams is mobilized (Dhillon and Inamdar, 2014), and where preferential pathways from overland and direct percolation into the tiles can be a primary source in agricultural systems in the Midwest (Blair et al., 2021; Cain et al., 2022).

In the present study within CCW, a tile drained agricultural landscape, observations of DOC supply not keeping up with an increase in discharge is likely due to a deficit in tile-accessible water storage (Cain et al., 2022). To activate subsurface transport flow paths during a storm event, along with associated OC sources, both above-tile and below-tile soil water storage must be filled before water can be laterally connected to streams. This "filling and connecting" process can be slow and even unachievable over the course of a storm event, in the antecedently-dry, bare soil period when the water-table is typically low in agricultural uplands (Schilling et al., 2018). Such a condition can be characterized as a disconnectivity between upland subsurface soil C pools and the stream during a storm event. Taken together, this would result in a clockwise C-Q hysteresis pattern as was found for both POC and DOC with higher concentrations on rising limbs (Fig. 7).

4.4.2. The "rapid growth" period exhibits progressive leaching of DOC

The counterclockwise patterns of C_{DOC}-Q, observed herein, indicate DOC contributors on the falling limb contained higher DOC than those on the rising limb - a situation reported by other studies as an accretion pattern resulting from sources that are later activated in the storm and/or distal from stream sampling point (Dhillon and Inamdar, 2014; Ramos et al., 2015; Vaughan et al., 2017; Liu et al., 2021; Rose and Karwan, 2021).

For the June 2016 CCW event, we propose that progressive leaching of DOC from soil explains the counterclockwise C_{DOC}-Q pattern (Fig. 8). June, is in general when most of the crops in CCW are in the rapid-growing stage, are near to full shielding capacity, and exhibit high evapotranspiration and water uptake rates, and when taken together all attenuate surface transport pathways for DOC (Blair et al., 2021). Further, we propose the DOC leachates from soil would be transported through a subsurface flow system that includes tile drains, in keeping with findings from Schilling et al. (2012) related to CCW. Extending the concept of above-tile and below-tile threshold of tile-runoff generation to this scenario, activation of various DOC sources is controlled by the generation of sufficient transferring flows up to the point when landscape soil water storage has been progressively filled (Cain et al., 2022).

4.5. Implications of findings to downstream evolution of fluvial OC

Clear Creek Watershed, Iowa can serve as a model for numerous US Midwestern watersheds to study export and evolution of upland/upstream OC as this system contains a number of typic geomorphic, sedimentological, and land use transitions along its flow paths, given its glacial origins, land use history, decreased hydrological connectivity from agricultural headwaters to its lower reaches, and increased forest riparian zone and urbanization at the watershed outlet (Fig. 1a; Blair et al., 2021). Estimating the degree of (dis)connectivity between hillslope and riparian area/stream would require further investigation on all potential DOC/POC sources within the different landscape units. Using POC $\delta^{13}C$ and biomarker measurements (e.g., lignin phenols), previous studies (Kim et al., 2020; Blair et al., 2021), highlighted that the CCW October event was characterized by an early pulse of corn-derived OC, which was delivered during the rising limb in the headwaters (i.e., S. Amana) and arrived at the lower reaches (i.e., Coralville) during the falling limb. Since our C_{DOC}-Q closely resemble C_{POC}-Q in Blair et al. (2021) for event #5, we speculate that a similar early mobilization of DOC would carry a strong corn signal from upland row crop downstream. Such a rapid delivery of upland OC might fuel subsequent biological processes downstream and within the inland aquatic system (Berhe et al., 2012). The highly disproportionate export of fluvial carbon during storm events identified herein should influence many subsequent biogeochemical processes in floodplains, streambed, inland, and coastal water bodies, with important implications for our estimates of the fluvial OC export and contribution to the atmospheric CO_2 (Stanley et al., 2012; Field and Barros, 2014).

5. Conclusion

Globally, row crop agriculture and the associated hydrologic management have dramatically altered both surface and subsurface flow pathways compared to the pre-settlement landscapes. This is particularly true in the central and upper Midwest USA where storm events provide frequent, flashy responses in low relief, naturally poorly drained watersheds, and facilitate rapid mobilization of terrestrial OC through expanded fluvial networks. Expanding upon our previous work exploring storm-event driven POC (Blair et al., 2021), we provide findings based on a high-resolution study of fluvial OC (both POC and DOC) in the agriculturally dominated Clear Creek Watershed (CCW) of eastern Iowa, USA.

We demonstrated a greater dominance of POC over DOC during the high-flow (storm) periods where the event-induced POC accounted for 54–94 % of total fluvial OC export. Extrapolation of a data treatment of our observation applying a hypothetical periodic monthly-only sampling of fluvial OC export would under-evaluate POC export by a factor of 1.9–5.4 fold because high POC concentrations during high-flow periods would be missed. This sampling bias perspective sheds a critical light on the importance of high-resolution analysis and event-based monitoring approaches. The disparity between event-driven POC and DOC export also exhibited a seasonal effect, where event-driven POC:DOC ratio was low (1.3–1.7) for October events while June/July events yielded a much higher POC:DOC export ratio up to a value of 14.7. The six storm events monitored, albeit a limited data set, could be binned into two clusters, cluster 1 (a “bare soil” period) and cluster 2 (a crop “rapid growth” period), through an evaluation of the watershed NDVI and AP_{30} during the storms. The response of DOC within the two clusters highlights a potential strong interaction or competing influences between surface coverage of vegetation and antecedent watershed wetness that indicates a seasonal shift in DOC source and transport pathway driven primarily by the degree of vegetation coverage/growth. Additionally, intra-storm variations in OC concentration and C-Q hysteresis patterns all demonstrate a seasonally-dependent shift, which can be viewed as the rapid liberation of easily erodible DOC during the “bare soil” period, and a progressive leaching of terrestrial DOC during the “rapid growth” period. Our multi-proxy, high-resolution, event-driven analysis demonstrates both competing and reinforcing drivers for DOC and POC export that highlight mechanisms controlled by agricultural management, geomorphology, and climate.

Non-discrimination statement

The U.S. Department of Agriculture (USDA) prohibits discrimination in all its programs and activities on the basis of race, colour, national origin, age, disability, and where applicable, sex, marital status, familial status, parental status, religion, sexual orientation, genetic information, political beliefs, reprisal, or because all or part of an individual's income is derived from any public assistance program. USDA is an equal opportunity provider and employer.

CRediT authorship contribution statement

Tingyu Hou: Writing – original draft, Analytical Work, Data Treatment, Data Curation. **Tim Filley:** Funding Acquisition, Conceptualization, Methods, Writing – review & editing, Project Administration, Supervision. **Neal Blair:** Funding Acquisition, Conceptualization, Methods, Writing – review & editing. **Thanos Papanicolaou:** Funding Acquisition, Conceptualization, Methods, Writing – review & editing.

Data availability

Data will be made available on request.

Declaration of competing interest

The authors declare that they have no known competing financial interests or personal relationships that could have appeared to influence the work reported in this paper.

Acknowledgements

This research was supported by National Science Foundation [grant number EAR1331906] for the Intensively Managed Landscape Critical Zone Observatory (IML-CZO) and [grant number EAR2012850] for Network Cluster CINet: Critical Interface Network in Intensively Managed Landscapes, a multi-institutional collaborative effort. The authors would like to thank Caroline Davis, Kara Prior, and Courtney Cappalli for their assistance with field sample collection, Jessie Moravek, Paul Roots, Yue Zeng, Dana Cooperberg, and Koushik Dutta assisted with DOC separation and POC analyses, and Jani Sparks for assistance with DOC processing and analysis.

Appendix A. Supplementary data

Supplementary data to this article can be found online at https://doi.org/10.1016/j.scitotenv.2023.161647.

References

Abaci, O., Papanicolaou, A.T., 2009. Long-term effects of management practices on water-driven soil erosion in an intense agricultural sub-watershed: monitoring and modelling. Hydrol.Process.Int.J. 23 (19), 2818–2837.

Abban, B., Papanicolaou, A., Cowles, M., Wilson, C., Abaci, O., Wacha, K., et al., 2016. An enhanced bayesian fingerprinting framework for studying sediment source dynamics in intensively managed landscapes. Water Resour. Res. 52 (6), 4646–4673.

Alvarez-Cobelas, M., Angeler, D., Sánchez-Carrillo, S., Almendros, G., 2012. A worldwide view of organic carbon export from catchments. Biogeochemistry 107 (1), 275–293.

Amado, A.A., Schilling, K., Jones, C., Thomas, N., Weber, L., 2017. Estimation of tile drainage contribution to streamflow and nutrient loads at the watershed scale based on continuously monitored data. Environ. Monit. Assess. 189 (9), 1–13.

Bagnold, R.A., 1966. An Approach to the Sediment Transport Problem From General Physics. US Government Printing Office.

Baker, D.B., Richards, R.P., Loftus, T.T., Kramer, J.W., 2004. A new flashiness index: characteristics and applications to midwestern rivers and streams 1. JAWRA J. Am. Water Resour. Assoc. 40 (2), 503–522.

Battin, T.J., Kaplan, L.A., Findlay, S., Hopkinson, C.S., Marti, E., Packman, A.I., et al., 2008. Biophysical controls on organic carbon fluxes in fluvial networks. Nat. Geosci. 1 (2), 95–100.

Baumann, M.S., Moran, S.B., Lomas, M.W., Kelly, R.P., Bell, D.W., 2013. Seasonal decoupling of particulate organic carbon export and net primary production in relation to sea-ice at the shelf break of the eastern Bering Sea: implications for off-shelf carbon export. J. Geophys. Res. Oceans 118 (10), 5504–5522.

Berhe, A.A., Harden, J.W., Torn, M.S., Kleber, M., Burton, S.D., Harte, J., 2012. Persistence of soil organic matter in eroding versus depositional landform positions. J. Geophys. Res. Biogeosci. 117 (G2).

Bettis, E.A., Muhs, D.R., Roberts, H.M., Wintle, A.G., 2003. Last glacial loess in the conterminous USA. Quat. Sci. Rev. 22 (18–19), 1907–1946.

Blair, N.E., Bettis III, E.A., Filley, T.R., Moravek, J.A., Papanicolaou, A., Ward, A.S., et al., 2021. The spatiotemporal evolution of storm pulse particulate organic carbon in a low gradient,agriculturally dominated watershed. Front. Water 3, 9.

Blume, T., Zehe, E., Bronstert, A., 2007. Rainfall—runoff response, event-based runoff coefficients and hydrograph separation. Hydrol. Sci. J. 52 (5), 843–862.

Boryan, C., Yang, Z., Mueller, R., Craig, M., 2011. Monitoring US agriculture: the US department of agriculture, national agricultural statistics service, cropland data layer program. Geocarto Int. 26 (5), 341–358.

Cai, Y., Guo, L., Douglas, T.A., 2008. Temporal variations in organic carbon species and fluxes from the Chena River,Alaska. Limnol. Oceanogr. 53 (4), 1408–1419.

Cain, M.R., Woo, D.K., Kumar, P., Keefer, L., Ward, A.S., 2022. Antecedent conditions control thresholds of tile-runoff generation and nitrogen export in intensively managed landscapes. Water Resour. Res. 58 (2), e2021WR030507.

Carlson, T.N., Ripley, D.A., 1997. On the relation between NDVI, fractional vegetation cover, and leaf area index. Remote Sens. Environ. 62 (3), 241–252.

Caverly, E., Kaste, J.M., Hancock, G.S., Chambers, R.M., 2013. Dissolved and particulate organic carbon fluxes from an agricultural watershed during consecutive tropical storms. Geophys. Res. Lett. 40 (19), 5147–5152.

Cerro, I., Sanchez-Perez, J.M., Ruiz-Romera, E., Antigüedad, I., 2014. Variability of particulate (SS, POC) and dissolved (DOC, NO3) matter during storm events in the Alegria agricultural watershed. Hydrol. Process. 28 (5), 2855–2867.

Cole, J.J., Prairie, Y.T., Caraco, N.F., McDowell, W.H., Tranvik, L.J., Striegl, R.G., et al., 2007. Plumbing the global carbon cycle: integrating inland waters into the terrestrial carbon budget. Ecosystems 10 (1), 172–185.

Dalzell, B.J., Filley, T.R., Harbor, J.M., 2005. Flood pulse influences on terrestrial organic matter export from an agricultural watershed. J. Geophys. Res. Biogeosci. 110 (G2).

Dalzell, B.J., Filley, T.R., Harbor, J.M., 2007. The role of hydrology in annual organic carbon loads and terrestrial organic matter export from a midwestern agricultural watershed. Geochim. Cosmochim. Acta 71 (6), 1448–1462.

Dalzell, B.J., King, J.Y., Mulla, D.J., Finlay, J.C., Sands, G.R., 2011. Influence of subsurface drainage on quantity and quality of dissolved organic matter export from agricultural landscapes. J. Geophys. Res. Biogeosci. 116 (G2).

De Rosa, P., Fredduzzi, A., Cencetti, C., 2019. Stream power determination in gis: an index to evaluate the most'Sensitive'points of a river. Water 11 (6), 1145.

Dhillon, G.S., Inamdar, S., 2014. Storm event patterns of particulate organic carbon (POC) for large storms and differences with dissolved organic carbon (DOC). Biogeochemistry 118 (1), 61–81.

Drake, T.W., Raymond, P.A., Spencer, R.G., 2018. Terrestrial carbon inputs to inland waters: a current synthesis of estimates and uncertainty. Limnol. Oceanogr. Lett. 3 (3), 132–142.

Elhakeem, M., Papanicolaou, A.T., Wilson, C.G., Chang, Y.-J., Burras, L., Abban, B., et al., 2018. Understanding saturated hydraulic conductivity under seasonal changes in climate and land use. Geoderma 315, 75–87.

Fabre, C.M., Sauvage, S., Tananaev, N., Noël, G.E., Teisserenc, R., Probst, J.-L., Pérez, J.S., 2019. Assessment of sediment and organic carbon exports into the Arctic ocean: the case of the Yenisei River basin. Water Res. 158, 118–135.

Fellman, J.B., D'Amore, D.V., Hood, E., 2008. An evaluation of freezing as a preservation technique for analyzing dissolved organic C, N and P in surface water samples. Sci. Total Environ. 392 (2–3), 305–312. https://doi.org/10.1016/j.scitotenv.2007.11.027.

Field, C.B., Barros, V.R., 2014. Climate Change 2014–Impacts, Adaptation and Vulnerability: Regional Aspects. Cambridge University Press.

Garcia, M., Peters-Lidard, C.D., Goodrich, D.C., 2008. Spatial interpolation of precipitation in a dense gauge network for monsoon storm events in the southwestern United States. Water Resour. Res. 44 (5).

Hedges, J.I., Keil, R.G., Benner, R., 1997. What happens to terrestrial organic matter in the ocean? Org. Geochem. 27 (5–6), 195–212.

Hernes, P.J., Spencer, R.G., Dyda, R.Y., Pellerin, B.A., Bachand, P.A., Bergamaschi, B.A., 2008. The role of hydrologic regimes on dissolved organic carbon composition in an agricultural watershed. Geochim. Cosmochim. Acta 72 (21), 5266–5277.

Hilton, R.G., Galy, A., Hovius, N., Horng, M.-J., Chen, H., 2010. The isotopic composition of particulate organic carbon in mountain rivers of Taiwan. Geochim. Cosmochim. Acta 74 (11), 3164–3181.

Hou, T., Filley, T.R., Tong, Y., Abban, B., Singh, S., Papanicolaou, A.T., et al., 2021. Tillage-induced surface soil roughness controls the chemistry and physics of eroded particles at early erosion stage. Soil Tillage Res. 207, 104807.

Inamdar, S., Singh, S., Dutta, S., Levia, D., Mitchell, M., Scott, D., Bais, H., McHale, P., 2011. Fluorescence characteristics and sources of dissolved organic matter for stream water during storm events in a forested mid-Atlantic watershed. J. Geophys. Res. Biogeosci. 116 (G3).

Jeong, J.J., Bartsch, S., Fleckenstein, J.H., Matzner, E., Tenhunen, J.D., Lee, S.D., et al., 2012. Differential storm responses of dissolved and particulate organic carbon in a mountainous headwater stream, investigated by high-frequency, in situ optical measurements. J. Geophys. Res. Biogeosci. 117 (G3).

Kim, J., Blair, N., Ward, A., Goff, K., 2020. Storm-induced dynamics of particulate organic carbon in Clear Creek, Iowa: an intensively managed landscape critical zone observatory story. Front. Water 2, 578261. https://doi.org/10.3389/frwa.

Lambert, T., Pierson-Wickmann, A.-C., Gruau, G., Jaffrézic, A., Petitjean, P., Thibault, J.-N., Jeanneau, L., 2014. DOC sources and DOC transport pathways in a small headwater catchment as revealed by carbon isotope fluctuation during storm events. Biogeosciences 11 (11), 3043–3056.

Lambert, T., Bouillon, S., Darchambeau, F., Morana, C., Roland, F.A., Descy, J.-P., Borges, A.V., 2017. Effects of human land use on the terrestrial and aquatic sources of fluvial organic matter in a temperate river basin (The Meuse River, Belgium). Biogeochemistry 136 (2), 191–211.

Larsen, S., Andersen, T., Hessen, D.O., 2011. Climate change predicted to cause severe increase of organic carbon in lakes. Glob. Chang. Biol. 17 (2), 1186–1192.

Larsen, S., Andersen, T., Hessen, D.O., 2011. Predicting organic carbon in lakes from climate drivers and catchment properties. Glob. Biogeochem. Cycles 25 (3).

Liu, W., Birgand, F., Tian, S., Chen, C., 2021. Event-scale hysteresis metrics to reveal processes and mechanisms controlling constituent export from watersheds: a review. Water Res. 200, 117254. https://doi.org/10.1016/j.watres.2021.117254.

Lloyd, C.E., Freer, J.E., Johnes, P.J., Collins, A., 2016. Testing an improved index for analysing storm discharge–concentration hysteresis. Hydrol. Earth Syst. Sci. 20 (2), 625–632.

Mu, C., Zhang, F., Chen, X., Ge, S., Mu, M., Jia, L., et al., 2019. Carbon and mercury export from the Arctic rivers and response to permafrost degradation. Water Res. 161, 54–60.

Mzobe, P., Berggren, M., Pilesjö, P., Lundin, E., Olefeldt, D., Roulet, N.T., Persson, A., 2018. Dissolved organic carbon in streams within a subarctic catchment analysed using a GIS/remote sensing approach. PLoS One 13 (7), e0199608.

Oeurng, C., Sauvage, S., Coynel, A., Maneux, E., Etcheber, H., Sánchez-Pérez, J.M., 2011. Fluvial transport of suspended sediment and organic carbon during flood events in a large agricultural catchment in southwest France. Hydrol. Process. 25 (15), 2365–2378.

Papanicolaou, A.N., Abban, B.K., Dermisis, D.C., Giannopoulos, C.P., Flanagan, D.C., Frankenberger, J.R., Wacha, K.M., 2018. Flow resistance interactions on hillslopes with heterogeneous attributes: effects on runoff hydrograph characteristics. Water Resour. Res. 54 (1), 359–380.

Papanicolaou, A.T., Wilson, C.G., Abaci, O., Elhakeem, M., Skopec, M., 2009. SOM loss and soil quality in the Clear Creek, IA. J.Iowa Acad.Sci. 116 (1–4), 14–26.

Papanicolaou, A.T., Wacha, K.M., Abban, B.K., Wilson, C.G., Hatfield, J.L., Stanier, C.O., Filley, T.R., 2015. From soilscapes to landscapes: a landscape-oriented approach to simulate soil organic carbon dynamics in intensively managed landscapes. J. Geophys. Res. Biogeosci. 120 (11), 2375–2401.

Papanicolaou, A.T.N., Elhakeem, M., Wilson, C.G., Burras, C.L., West, L.T., Lin, H.H., et al., 2015. Spatial variability of saturated hydraulic conductivity at the hillslope scale: understanding the role of land management and erosional effect. Geoderma 243, 58–68.

Pawson, R.R., Evans, M.G., Allott, T.E.H.A., 2012. Fluvial carbon flux from headwater peatland streams: significance of particulate carbon flux. Earth Surf. Process. Landf. 37 (11), 1203–1212.

Peacock, M., Freeman, C., Gauci, V., Lebron, I., Evans, C.D., 2015. Investigations of freezing and cold storage for the analysis of peatland dissolved organic carbon (DOC) and absorbance properties. Environ.Sci. Processes Impacts 17 (7), 1290–1301. https://doi.org/10.1039/c5em00126a.

Prior, J.C., 1991. Landforms of Iowa. University of Iowa Press.

Ramos, T., Rodrigues, S., Branco, M., Prazeres, A., Brito, D., Gonçalves, M., et al., 2015. Temporal variability of soil organic carbon transport in the Enxoé agricultural watershed. Environ. Earth Sci. 73 (10), 6663–6676.

Raymond, P.A., Saiers, J.E., 2010. Event controlled DOC export from forested watersheds. Biogeochemistry 100 (1), 197–209.

Raymond, P.A., Oh, N.-H., Turner, R.E., Broussard, W., 2008. Anthropogenically enhanced fluxes of water and carbon from the Mississippi River. Nature 451 (7177), 449–452.

Ren, Z., Niu, D., Ma, P., Wang, Y., Wang, Z., Fu, H., Elser, J.J., 2020. C: N: P stoichiometry and nutrient limitation of stream biofilms impacted by grassland degradation on the Qinghai-Tibet Plateau. Biogeochemistry 150 (1), 31–44.

Rochelle-Newall, E., Hulot, F.D., Janeau, J.L., Merroune, A., 2014. CDOM fluorescence as a proxy of DOC concentration in natural waters: a comparison of four contrasting tropical systems. Environ. Monit. Assess. 186 (1), 589–596.

Rose, L.A., Karwan, D.L., 2021. Stormflow concentration–discharge dynamics of suspended sediment and dissolved phosphorus in an agricultural watershed. Hydrol. Process. 35 (12), e14455.

Royer, T.V., David, M.B., Gentry, L.E., 2006. Timing of riverine export of nitrate and phosphorus from agricultural watersheds in Illinois: implications for reducing nutrient loading to the Mississippi River. Environ.Sci.Technol. 40 (13), 4126–4131.

Sanderman, J., Lohse, K.A., Baldock, J.A., Amundson, R., 2009. Linking soils and streams: sources and chemistry of dissolved organic matter in a small coastal watershed. Water Resour. Res. 45 (3).

Schilling, K.E., Jindal, P., Basu, N.B., Helmers, M.J., 2012. Impact of artificial subsurface drainage on groundwater travel times and baseflow discharge in an agricultural watershed, Iowa (USA). Hydrol. Process. 26 (20), 3092–3100.

Schilling, K.E., Streeter, M.T., Bettis III, E.A., Wilson, C.G., Papanicolaou, A.N., 2018. Groundwater monitoring at the watershed scale: an evaluation of recharge and non-point source pollutant loading in the Clear Creek Watershed,Iowa. Hydrol. Process. 32 (4), 562–575.

Stanley, E.H., Powers, S.M., Lottig, N.R., Buffam, I., Crawford, J.T., 2012. Contemporary changes in dissolved organic carbon (DOC) in human-dominated rivers: is there a role for DOC management? Freshw. Biol. 57, 26–42.

USDA National Agricultural Statistics Service, 2017. Census of Agriculture. Complete data available at. www.nass.usda.gov/AgCensus.

Valayamkunnath, P., Barlage, M., Chen, F., Gochis, D., Franz, K., 2020. Mapping of 30-meter resolution tile-drained croplands using a geospatial modeling approach. Sci. Data 7, 257. https://doi.org/10.1038/s41597-020-00596.

Van Oost, K., Quine, T., Govers, G., De Gryze, S., Six, J., Harden, J., et al., 2007. The impact of agricultural soil erosion on the global carbon cycle. Science 318 (5850), 626–629.

Vaughan, M.C., Bowden, W.B., Shanley, J.B., Vermilyea, A., Sleeper, R., Gold, A.J., et al., 2017. High-frequency dissolved organic carbon and nitrate measurements reveal differences in storm hysteresis and loading in relation to land cover and seasonality. Water Resour. Res. 53 (7), 5345–5363.

Wacha, K.M., Papanicolaou, A., Giannopoulos, C.P., Abban, B.K., Wilson, C.G., Zhou, S., et al., 2018. The role of hydraulic connectivity and management on soil aggregate size and stability in the Clear Creek Watershed, Iowa. Geosciences 8 (12), 470.

Wacha, K.M., Papanicolaou, A.T., Abban, B.K., Wilson, C.G., Giannopoulos, C.P., Hou, T., et al., 2020. The impact of tillage row orientation on physical and chemical sediment enrichment. Agrosyst. Geosci. Environ. 3 (1), e20007.

Wilson, C.G., Papanicolaou, A.T., Denn, K.D., 2012. Partitioning fine sediment loads in a headwater system with intensive agriculture. J. Soils Sediments 12 (6), 966–981.

Wilson, C.G., Abban, B., Keefer, L.L., Wacha, K., Dermisis, D., Giannopoulos, C., et al., 2018. The intensively managed landscape critical zone observatory: a scientific testbed for understanding critical zone processes in agroecosystems. Vadose Zone J. 17 (1), 1–21.

Wilson, H.F., Xenopoulos, M.A., 2009. Effects of agricultural land use on the composition of fluvial dissolved organic matter. Nat. Geosci. 2 (1), 37–41.

Yang, Z., Yu, G., Di, L., Zhang, B., Han, W., Mueller, R., 2013. Web service-based vegetation condition monitoring system-vegscape. Paper Presented at the 2013 IEEE International Geoscience and Remote Sensing Symposium-IGARSS.

Yengoh, G.T., Dent, D., Olsson, L., Tengberg, A.E., Tucker, C.J., 2015. Introduction. In: Use of the Normalized Difference Vegetation Index (NDVI) to Assess Land Degradation at Multiple Scales. SpringerBriefs in Environmental Science. Springer, Cham. https://doi.org/10.1007/978-3-319-24112-8_1.